Journal of the Brazilian Society of Mechanical Sciences and Engineering (2019) 41:329
https://doi.org/10.1007/s40430-019-1829-1

TECHNICAL PAPER

Barkhausen noise signal of different steels upon face-turning process

Vineet Dawara[1] · **M. Vashista**[1] · **M. Z. KhanYusufzai**[1]

Received: 3 January 2019 / Accepted: 16 July 2019 / Published online: 23 July 2019

Abstract
This paper deals with understanding the effects of excitation field parameters on the nature of Barkhausen noise profile in order to improve the validity of Barkhausen noise results for the machining process. The experiment has been performed on total of four samples, two of high carbon steel and two of high carbon chromium steel. First, all samples are subjected to process annealing and later one sample of each steel was subjected to face-turning process. Barkhausen noise measurement was performed in two steps: first, magnetizing frequency varied and magnetic field intensity kept constant, and second, magnetic field intensity varied and magnetizing frequency kept constant. Magnetic Barkhausen noise profile is obtained by fitting Gaussian function to the root-mean-square distribution of the Barkhausen signal. The complicated behaviour of the profiles with frequency suggests optimum frequency determined statistically, which reflects the stochastic behaviour and can be applied to describe and control the face-turning process. The peak value of the profiles with amplitude of the sinusoidal magnetic field intensity has found to resemble exponential decay correlation.

Keywords Barkhausen noise signal · Face turning · Magnetic field intensity · Magnetizing frequency

1 Introduction

The first theoretical examination of the structure of a domain wall was made by Felix Bloch in 1932. This domain wall moves in response to the applied field, but its motion is observed to be jerky and discontinuous, rather than smooth. The first observation for this phenomenon dates back in 1919 by Heinrich Barkhausen, and hence the name Barkhausen effect, where he noticed that iron produces crackling noise on the speaker when magnetized no matter how smoothly and continuously the field is increased. If the pickup coil is connected to the oscilloscope, instead of speaker, irregular spikes will be observed on the voltage–time curve. These voltage spikes are called Barkhausen noise (BN) [1]. The electromotive force induced in the pickup coil is proportional to the rate of change of flux through it. The effect is strongest on the steepest portion of magnetic induction field (B) versus magnetic field intensity (H) curve, which is popularly known as hysteresis curve, and is evidence for sudden, discontinuous changes in magnetization [2, 3].

Magnetization can change as a result of domain wall motion and domain rotation. Wall motion is the main process up to about "knee" of the magnetization curve as shown in Fig. 1. From there to saturation, rotation predominates; in this region, work must be done against the anisotropy forces, and a rather large increase in H is required to produce a relatively small increase in B. But this division of the magnetization curve is rather arbitrary, because wall motion and rotation are not sharply divisible processes. In fact, at any one level of B, wall motion may be occurring in one portion of a specimen and rotation in another. When magnetization occurs entirely by domain rotation, we expect the process to be reversible, with same hysteresis curve followed in both increasing and decreasing fields. Domain wall motion in materials is irreversible, leading to different curves for increasing and decreasing fields [4]. The jerky motion of the domain wall is due to hindrances caused by inclusions like particles of a second phase in an alloy, oxide or sulphide particles, simply holes or cracks, etc. Residual stresses and microhardness also impede the motion. Thus, BN signal helps understand magnetization process and hysteretic properties on microscopic scale and a lot effort has been done to relate the phenomenology to the microscopic origin as it

Technical Editor: Marcelo Areias Trindade.

✉ M. Vashista
mvashista.mec@itbhu.ac.in

[1] Department of Mechanical Engineering, Indian Institute of Technology (BHU), Varanasi, India

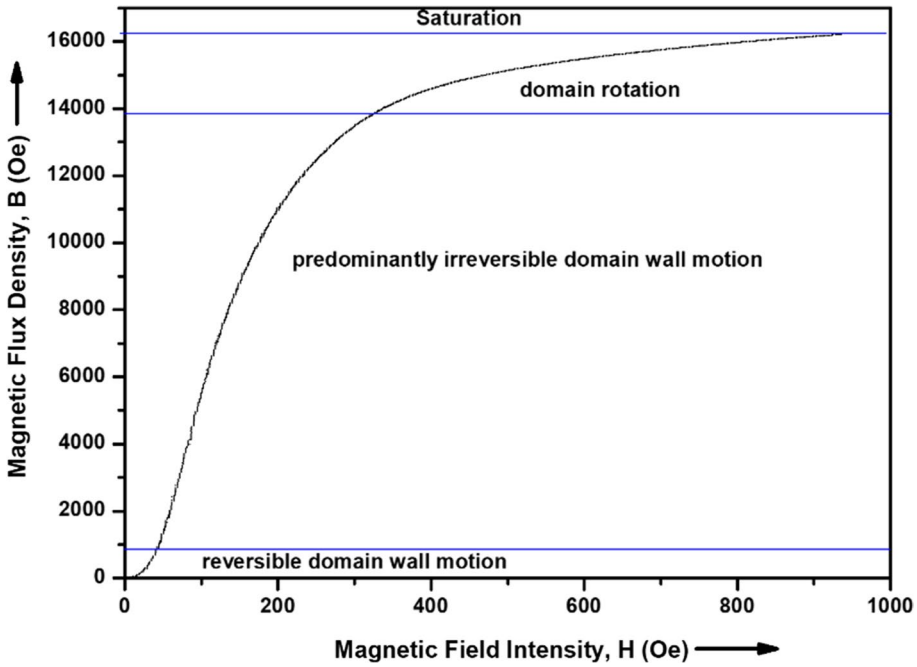

Fig. 1 Magnetization process showing domain wall motion and rotation

is sensitive to material microstructure, residual stress and surface microhardness. It is possible to obtain a stationary signal and perform the statistical analysis; thus, statistical properties of the noise can be described and controlled with some assumptions verified experimentally.

BN signal analysis has been a research topic in the literature to determine the surface-hardened depth by induction hardening [5], to study the effect of applied stress and residual stress due to plastic deformation on steels [6–8], to assess the microstructure changes during tempering [9] and ferrite proportion in dual-phase steels [10] and to characterize the pearlite grains in plain carbon steel [11]. Measurement and analysis of the BN envelope or root-mean-square (RMS) profile plotted against the applied voltage or current and its peak position and magnitude to related with the phenomenon.

BN energy has also been used as a parameter in the literature to relate some phenomena: residual stress [12], differential elastic and plastic deformation [13], stress concentration due to the presence of defects [14] and microstructural state of the ferrite stainless steel [15]. While some researchers have used frequency spectrum of the signal to study the effect of grain size and grain boundary disorientation on BN [16], different microstructural region in weld HAZ [17], to distinguish different constituent of steel [18].

Online monitoring of the grinding damage in gears using MBN technique has been successfully applied [19]. Few researchers have monitored the surface quality after milling process. Erik et al. [20] have monitored the milling surfaces of steel AISI SAE 1020, square solid bar 50 × 50 mm, using Barkhausen technique and found that cutting speed and roughness have strong correlation with MBN energy. Stupakov et al. [21] have applied Barkhausen noise for detection of milling-induced surface damage in a typical bearing steel 100Cr6.

Surface characteristics such as microhardness, roughness, residual stress and microstructure change during turning process as a consequence of the following factors: strain rate of local plastic deformation; high temperature developed; high cutting force; and chemical reaction between tool and workpiece, and the existence of the complex coupling among these factors makes the turning process highly nonlinear, and so thus the relationship between the surface characteristics and turning parameters. Residual stress, roughness and hardness that can be found in a mechanical part are also generated in the final steps of the machining process. If magnetic Barkhausen noise (MBN) technique can be used to analyse these surface characteristics which are used for quality control of a machining process, then a portable quality control system can reduce the checking time of the process [19–22]. Martin et al. [22] have attempted to apply Barkhausen noise technique to analyse the surface quality after grinding and turning. Experiments were carried out on the roll bearing steel 100Cr6, made in the form of rings of external diameter 56 mm, internal diameter 40 mm and width 7 mm. These rings were ground and turned under the constant cutting conditions. The analysis of stress state showed that the conventional evaluation of Barkhausen noise could be applied to the identification of thermal load and hence the monitoring of a grinding process, while it failed in the monitoring of turning process due to more complicated variation in thermal and mechanical load.

The dependency of the MBN signal on the magnetic excitation parameter has further posed a complication to drive necessary information from the signal which can describe and control the machining process. Vashista and Moorthy [23] have studied the influence of applied magnetic field strength using two yokes of 14,000 A/m (176 Oe) and 22,000 A/m (276 Oe) on low-frequency (0.4 Hz) BN profile, and two peaks were observed with higher magnetic field strength of 276 Oe on quenched–tempered and case-carburised–tempered steels. They have extended their experiment by using high and low frequency for MBN measurement systems on samples of low carbon and high carbon steel. The high-frequency (= 125 Hz) MBN profile showed single peak for all the samples due to insufficient applied field strength (188 Oe) and shallow magnetic skin depth, whereas low-frequency (= 0.4 Hz) MBN profile showed two peaks due to greater magnetization inside the bulk material [24]. Magnetic Barkhausen noise signal at high frequency range should be obtained to derive necessary information of the surface inhomogeneities, caused by high cutting force and temperature due to local shear deformation at the tool–workpiece contact during machining. But, Blažek et al. [25] have analysed BN signal in high-frequency regimes (up to 1000 Hz) and inferred that data interpretation has much complexities due to variable ratios of thermal noise to BN noise as well as distortion of signal due to vibrations in high-frequency regime; thus, raw signal received and pure BN signal can differ remarkably. According to the Pérez-Benítez model [26], the MBN is produced by the interaction of domain walls with defects, where the coercive field of these defects follows a Gaussian distribution function. Chávez-González et al. [27] also proposed a model based on [26], but also took eddy currents into account.

Literature survey indicates that a limited work has been carried out on wide range of applied magnetic field strengths and excitation frequencies, and a handful of researchers have worked to apply magnetic Barkhausen noise technique to analyse the surface integrity after machining. In the present paper, a statistical method is presented in which magnetic Barkhausen noise profile is obtained by fitting single-peak Gaussian function to the moving RMS distribution of the obtained raw signal and the effect of wide range of both magnetizing frequencies and magnetic field intensities on the parameters (peak height and position) of the magnetic Barkhausen noise profile has been briefly studied. The aspects from application point of view of the obtained profile to describe the change in surface characteristics, caused by face turning, are discussed that cause the change in parameters of the MBN profile, obtained at optimum frequency determined statistically.

2 Materials and method

2.1 Experimental process and measurements

Four workpieces of disc shape, of diameter 140 mm and of thickness 15 mm were taken. Each was process annealed to relieve internal stress under the condition shown in Table 1. Out of four, two discs (marked as PA1 and PAM1) are of high carbon high chromium steel having hardness around 211 BHN and remaining two (marked as PA2 and PAM2) are of high carbon steel having hardness around 187 BHN. Hence, two different steels were used for the experiment. Further, one disc out of two of particular steel (i.e., PAM1 and PAM2) was subjected to facing in lathe, by tool with CVD coating of TiN–TiCN–Al_2O_3–TiN, whose designation is shown in Table 2, with experimental condition. This cutting parameters and tool were chosen to obtain smooth surface finish, followed by surface abrasion with emery paper of 400 to 2000 mesh numbers prior to magnetic Barkhausen noise testing such that effect of surface roughness on the signal is negligible and micro-air gaps is avoided.

Barkhausen noise testing was performed by Magstar magnetic Barkhausen noise sensor and software package developed by CSIR-NML, Jamshedpur, India, in which a sinusoidal cyclic magnetic field up to 1500 Oe with an excitation frequency of 10–200 Hz can be induced for Barkhausen signal with variable band-pass filter within 10–300 kHz shown in Fig. 2. Magnetic field intensity (H) is basically an excitation field, and the parameters: frequency and amplitude, of this field can easily be controlled. Therefore, the test was conducted in two steps, first by varying magnetizing frequencies from 10 to 200 Hz and keeping amplitude of the magnetic field intensity constant equal to 300 Oe and second by varying amplitude of magnetic field intensity from 100 to 800 Oe and keeping frequency constant to 25 Hz. The

Table 2 Experimental conditions for machining operation

Tool	Insert designation: DMMG150608TN200 Holder designation: PDJNR 2020 K15 WIDAX
Operation	Dry facing in three passes
Cutting parameters	RPM = 1000, feed = 0.227 mm/rev, DoC = 0.2 mm

Table 1 Conditions for process annealing

Heating	Holding	Cooling
Heated in furnace up to 600 °C	Held at that temperature for 45 min	Cooled in furnace for 45 min and then in still air

Fig. 2 Magstar MBN sensor and software package

orientation and position of the sensor are shown in Fig. 3. The sensor was placed at radius of 45 mm on the disc surface, and data were recorded for three cycles of excitation field.

2.2 Post-processing analysis of raw data

For one complete cycle of *B–H* curve, corresponding two bursts are obtained as illustrated in Fig. 4. Burst 1 occurs when magnetization takes place in positive direction, i.e., when *B–H* curve follows path d–e–f–a, and burst 2 occurs when magnetization takes place in negative direction, that is, when *B–H* curve follows path a–b–c–d. Since three cycles of the excitation field are applied, a total of six bursts are obtained as shown in Fig. 5a.

The bursts 1, 3 and 5 are obtained when magnetization takes place in positive direction (Fig. 4), and bursts 2, 4 and 6 are obtained when magnetization takes place in negative direction. The *n*th moving RMS distribution (n can be any positive integer) of obtained raw data was calculated using the equation, defined as:

$$V_{k,\mathrm{rms}} = \sqrt{\frac{1}{n}\sum_{i=k-n}^{i=k} V_i^2}$$

where V_i is raw BN signal and k varies from 1 to N (N is total numbers of data values). This was done to obtain only positive signal and also to minimize background noises captured during measurements. The filtered MBN signal obtained is also shown in Fig. 5a. Then, the bursts 1, 3 and 5 are averaged corresponding to positive magnetization. The filtered signal obtained from the successive steps so far is curve fitted with single peak with Gaussian distribution with Levenberg–Marquardt algorithm (LMA) as shown in Fig. 5b. LMA is a standard iterative technique to solve nonlinear least square problems, typically those of curve fitting in which nonlinear function is fitted to a set of measured data points by minimizing the sum of the squares of the errors between the function and the measured data points [28]. Single peak is expected because process annealing and facing would not cause any profound phase change from surface to the bulk.

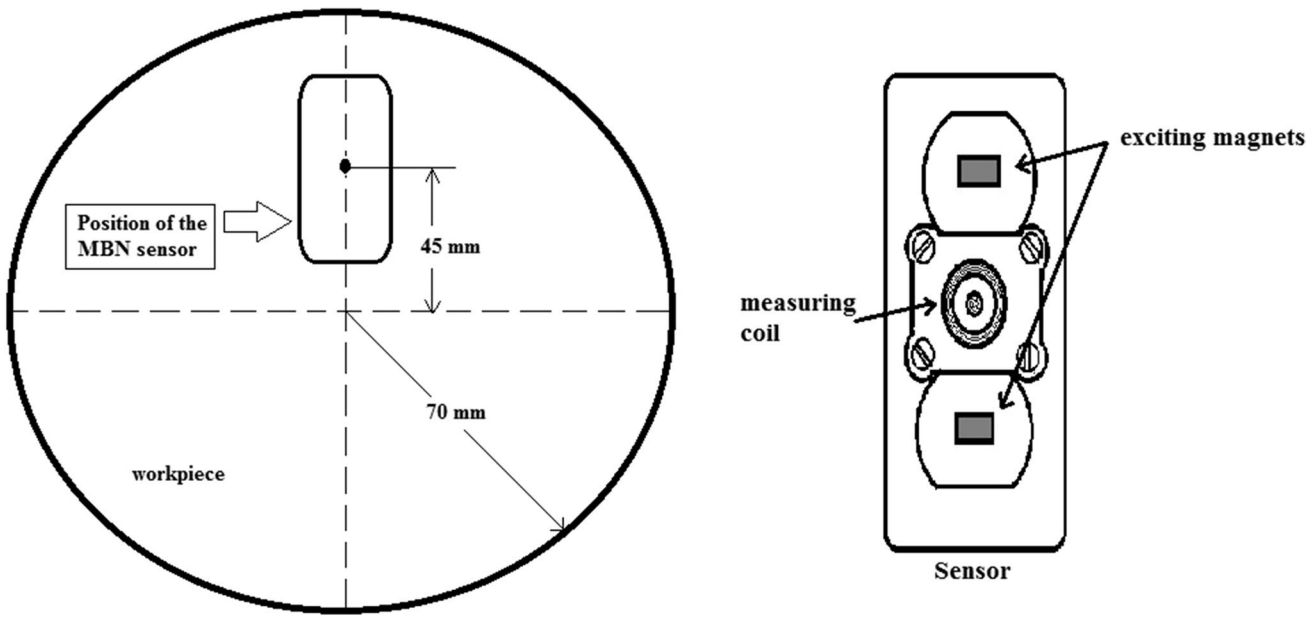

Fig. 3 Position and orientation of the magnetic Barkhausen noise sensor

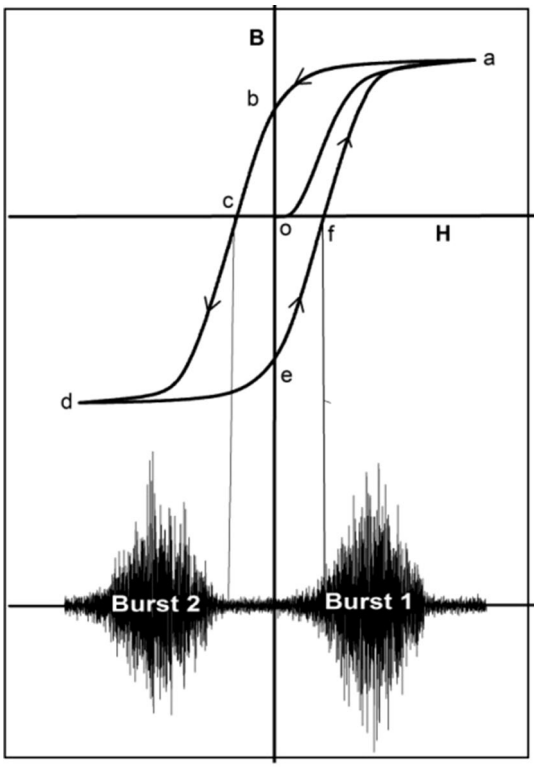

Fig. 4 *B–H* curve and corresponding magnetic Barkhausen noise bursts obtained

3 Results and discussions

3.1 Effect of frequency on the MBN profile

Since time period (T) for half-sinusoidal waveform of applied magnetic field depends on its frequency, non-dimensionalized time (t^*) was introduced to club all the curves of different frequencies into single plot shown in Figs. 6, 7 and 8. t^* is calculated as ratio of actual time (t) to half of the time period (T) at that frequency. It was found to be convenient way to represent the variation in the exciting field along the abscissa. So in brief, as t varies from 0 to $T/2$ for half cycle, t^* varies from 0 to 1; consequently, sinusoidal exciting field varies from zero to maximum and again decreases to zero completing one half cycle. At $t^* = 0.5$, the excitation field takes its maximum value equal to amplitude.

Figure 6a, b shows the MBN profiles for the sample PA_1 and PA_M1. The MBN profiles obtained at different frequencies behave in similar way for both machined and un-machined samples. The peak value of the profiles decreases with frequency of the excitation field, and it is highest when frequency equals 25 Hz for both the samples. Figures 7 and 8 show the MBN profiles for the samples PA_2 and PA_M2, in which peak value of the fitted profiles first increases and then decreases with frequency of the excitation field, and it is highest when frequency equals 50 Hz for both the samples. It is evident as there is optimum frequency at which the signal has maximum strength because MBN signal, according to Faraday's law, is given as $v_{\mathrm{MBN}} = -nS\frac{\mathrm{d}B}{\mathrm{d}t}$, where $B = \mu_o(H + M)$ is magnetic induction field, and the peak value depends upon two factors: the rate of change of magnetic field intensity $\frac{\mathrm{d}H}{\mathrm{d}t} = 2\pi f H_a \cos(2\pi t^*)$, which increases with frequency as H_a, which is the amplitude of the magnetic field intensity, is constant and the rate of change of magnetization $\frac{\mathrm{d}M}{\mathrm{d}t} \propto$ (domain wall velocity), which decreases with frequency due to proportional increase in coercive field of the pinning sites as a result of induced eddy current in the specimen [27, 29]. The peak occurs before $t^* < 0.5$ for all the samples that is along the path f–a in *B–H* curve (refer Fig. 4). The peak position of the magnetic Barkhausen noise signal profile shifts slightly to the right with

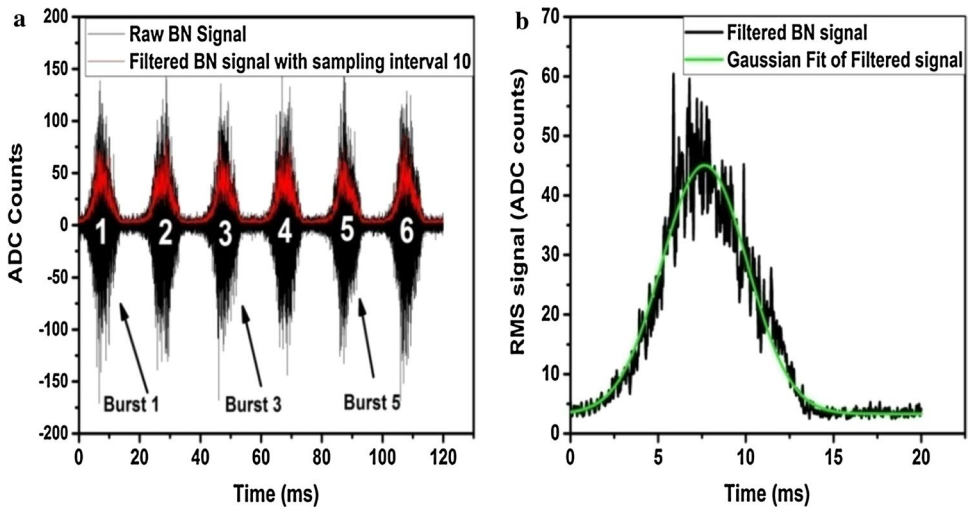

Fig. 5 Measured MBN signal along with filtered signal in (**a**) at 25 Hz frequency for disc PA_1 and Gaussian fit in (**b**)

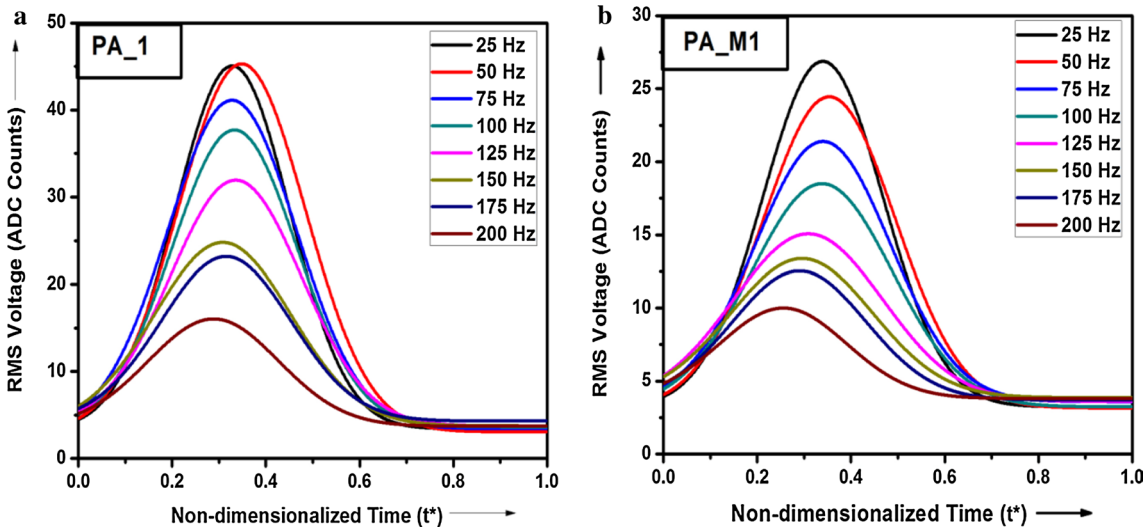

Fig. 6 Effect of frequency on RMS profile on discs **a** PA_1, **b** PA_M1, at constant amplitude of magnetic field intensity = 300 Oe

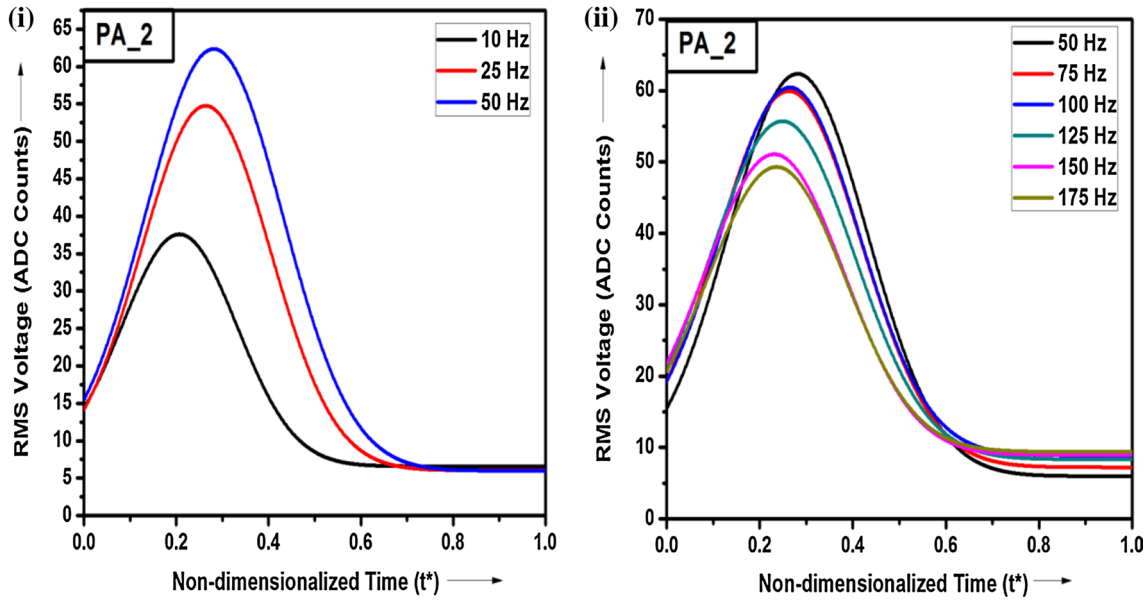

Fig. 7 Effect of frequency on RMS profile on disc PA_2 at constant amplitude of magnetic field intensity = 300 Oe, when frequency varies from (i) 10 to 50 Hz, (ii) 50 to 175 Hz

increasing frequency up to 50 Hz and then shifts slightly to the left for all samples. Apart from induced eddy current, the behaviour of the magnetic Barkhausen noise signal profile with frequency is further complicated due to increased background noises, vibrations and magnetic damping at higher frequencies [25]. The R^2 value falls from 0.95 for 25 Hz to 0.65 for 200 Hz, indicating Gaussian fitting of the RMS data of the MBN signal best reflects the stochastic nature of Barkhausen jumps at frequency less than or equal to 50 Hz for all samples as the R^2 value is greater than 0.90 in this frequency range.

Peak positions in terms of t^* and respective magnetic field intensity (H) values corresponding to optimum frequency are tabulated in Table 3 for all samples. It is to be noted that face turning of the samples has two effects: attenuation of the signal peak and also increase in peak position indicating slight delay in peak value. At same frequency and amplitude of the magnetic field intensity, the

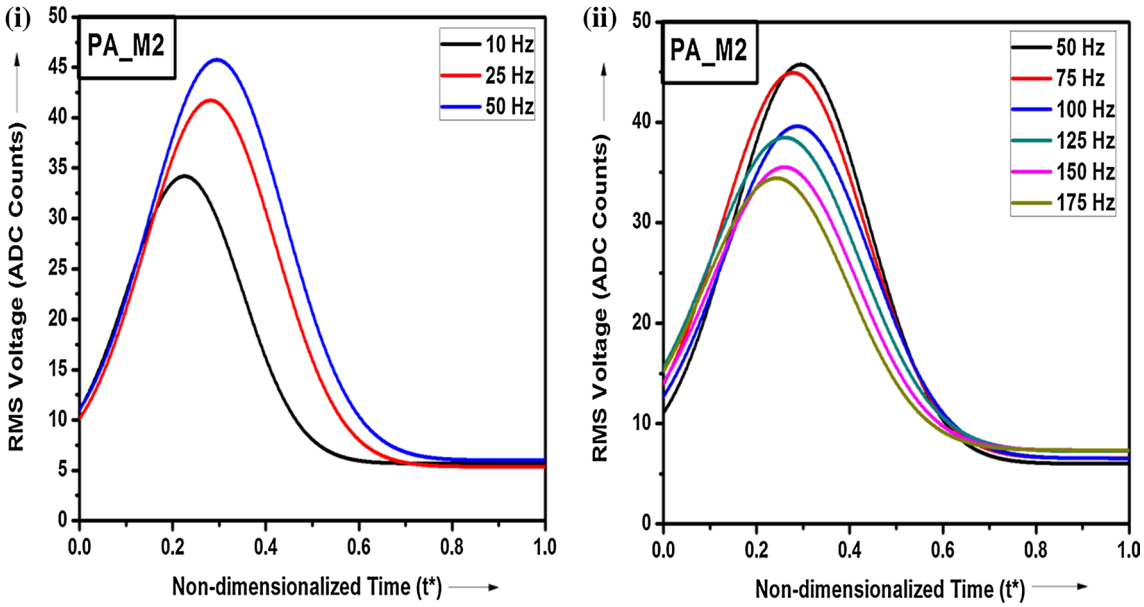

Fig. 8 Effect of frequency on RMS profile on disc PA_M2 at constant amplitude of magnetic field intensity = 300 Oe, when frequency varies from (i) 10 to 50 Hz, (ii) 50 to 175 Hz

Table 3 Peak value and peak position of BN profiles

	PA_1	PA_M1	PA_2	PA_M2
Optimum frequency	25 Hz	25 Hz	50 Hz	50 Hz
Peak value (ADC counts)	45.08668	26.87873	62.34701	45.76033
Peak position (t^*)	0.32824	0.34025	0.28121	0.29522
Peak position (MFI)	257.3747 Oe	263.0058 Oe	231.8796 Oe	240.0302 Oe
XRD data (2-theta)	44.753	44.552	44.4408	44.5421

faced samples PA_M1 and PA_M2 show decrease in peak value and increase in peak position with respect to samples PA1 and PA2, respectively, as a result of change in surface characteristic after face turning. It is observed that no such microstructural change has been caused at this cutting speed of the specimen, but the X-ray diffraction perpendicular to the surface result shows the shift in 2-theta value of the maximum intensity (refer Table 3), indicating change in residual stress. According to the Bragg's law, decrease in 2-theta value will result in increase in interplanar spacing, implying positive strain perpendicular to the surface and negative strain along the surface due to state of plane stress [30]. Peak height is closely related to the stress change within the material [7, 8] and negative stress reduces the peak height, so the 2-theta value should decrease, but result is bit controversial for PA_M2. The reason for that may be that all material properties affect the signal and that the other properties affect the magnetic Barkhausen noise signal more than residual stress, so the unmeasured properties may cloud the effect and even change the direction of the effect. Peak position is stated to be closely related to coercivity and also to the hardness [8, 9]. So, the increase in peak position implies higher surface hardness, consequently due to work hardening of the machined surface.

3.2 Effect of magnetic field intensity on MBN profile

There is no need for non-dimensionalized parameter because of constant time period of 20 ms. Figure 9 shows the MBN profiles at different amplitudes of magnetic field intensity for all the samples and peak value increases with increase in amplitude, whereas peak position decreases. It is obvious as the domain wall velocity increases, consequently increasing $\frac{dM}{dt}$ along with the term $\frac{dH}{dt}$, with increase in amplitude of magnetic field intensity. Peaks are also obtained earlier as the specimen attains the state of magnetic saturation due to easy unpinning motion of the domain wall. It also demonstrates the fact that random distributions of local pinning sites are progressively exceeded by the higher amplitude of the magnetic field intensity [31]. The R^2 coefficient for all Gaussian profile of the RMS distribution of Magnetic Barkhausen noise signal is between 0.89 and 0.94, indicating

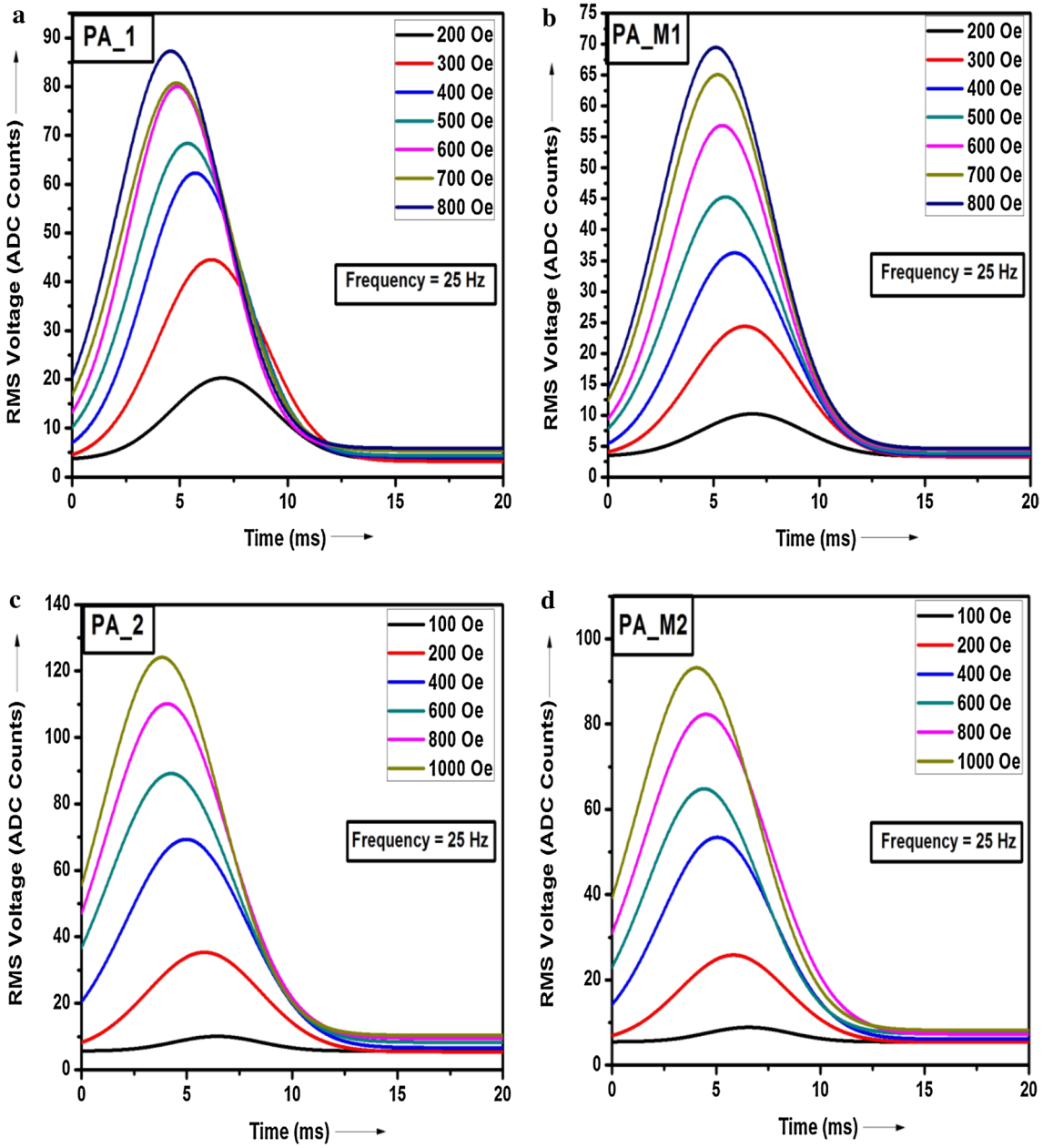

Fig. 9 Effect of magnetic field intensity on BN profile for **a** PA_1, **b** PA_M1, **c** PA_2 and **d** PA_M2

that the profile reflect the domain wall dynamics, but Chi square value (X^2) drastically increases with amplitude of the magnetic field intensity, implies error due to difference between actual RMS value and RMS value predicted by the fitted Gaussian curve also increases.

Again, the comparison of the profiles, shown in Fig. 10, shows that the magnitude of the peak value is lesser, and peak position is delayed for machined samples compared to un-machined samples. The exciting relationship in Fig. 11 shows that the variation in the peak values of the MBN signal exactly follows exponential decay function, $v_{\text{peak}} = v_0 + A\exp(-H_0/k)$, with R^2 coefficient value of 0.99 of the fitted curve. As H_0 tends to zero, v_{peak} should tend to zero, but no peaks were obtained for $H_o < 200Oe$. This function only has physical meaning for $H_o \geq 200Oe$. The constants k (decay constant) and A of the decay function, tabulated in Table 4, have larger value for machined samples depicting the dependence on the material and process history, but exact interpretation of this function still requires further research.

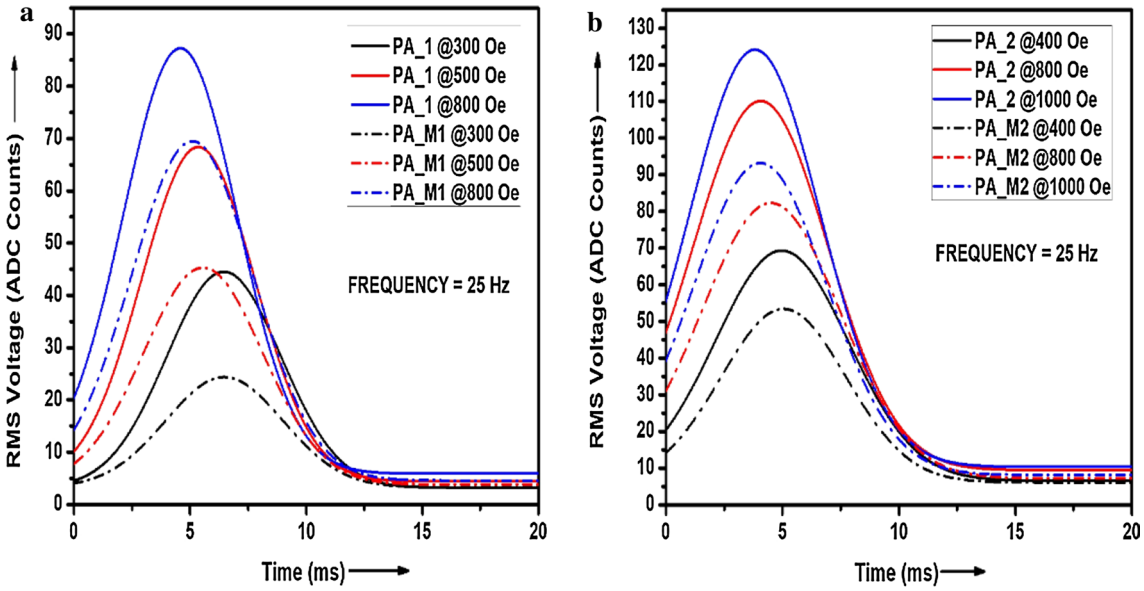

Fig. 10 Comparison of RMS profiles obtained at constant excitation frequency, but varying magnetic field intensity between **a** PA_1 and PA_M1, **b** PA_2 and PA_M2

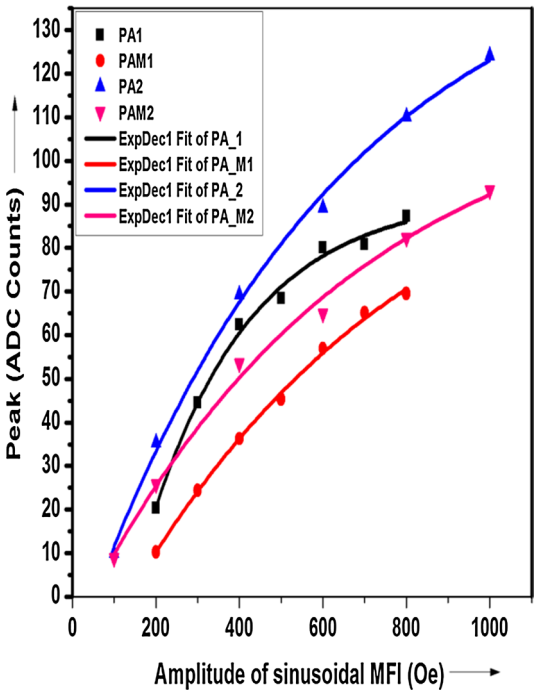

Fig. 11 Correlation of magnetic Barkhausen noise signal peak with amplitude of sinusoidal magnetic field intensity

Table 4 Constants of exponential decay function

Parameters	PA_1	PA_M1	PA_2	PA_M2
v_0	92.11	114.20	156.65	120.39
A	− 162.11	− 139.02	− 170.63	− 128.80
k	244.74	690.68	615.20	657.88

4 Conclusion

The Gaussian fitting of the moving RMS data of the MBN signal at optimum frequency determined statistically reflects the stochastic nature of the Barkhausen phenomenon pretty good as considering the challenges due to stochastic nature and its dependence on BN measurement equipment (pickup coil, probe, sensor, etc.) and specimen geometry, along with applied frequency and magnetic field intensity, have posed the necessity to determine magnetic excitation parameter such that the suitable information from the signal can be decoded to describe and control the machining process. The parameters of the MBN profile obtained can be studied to analyse surface characteristics of the face-turning process if all the material properties affecting the BN activity is measured. The exponential decay relationship between the MBN peak and the amplitude of the sinusoidal magnetic field intensity is difficult to generalize unless the experiment is conducted for a wide range of cutting conditions, necessitating further research.

Acknowledgements The authors gratefully acknowledge the funding support they received from IIT (BHU) under Institute Research Project (IIT (BHU)/R&D/IRP/2015-16/2832/L dated 31.12.2015).

References

1. Barkhausen H (1930) Whistling tones from earth. Proc Inst Radio Eng 18(7):1155–1159

2. Weigman NJ, Stege R (1978) Barkhausen effect in magnetic thin films: general behaviour and stationarity along the hysteresis loop. Appl Phys 16:167–174
3. Bertotti G, Fiorillo F (1981) Barkhausen noise and domain structure dynamics in SiFe at different points of the magnetization curve. J Magn Mater 23:136–148
4. Cullity BD, Graham CD (2009) Introduction to magnetic materials, vol 9. Wiley, Hoboken, pp 302–314
5. Saquet O, Tapuleasa D, Chicois J (1998) Use of Barkhausen Noise for determination of surface hardened depth. Nondestr Test Eval 14(5):277–292
6. Kleber X, Hug A, Merlin J (2005) Characterization of residual stresses in plastically deformed ferrite-martensite steels using Barkhausen noise measurements. Mater Sci Forum 500–501(205):655–662
7. Moorthy V, Shaw BA, Day S (2004) Evaluation of applied and residual stresses in case carburised En36 steel subjected to bending using the magnetic Barkhausen emission technique. Acta Mater 52:1927–1936
8. Stewart DM, Stevens KJ, Kaiser AB (2004) Magnetic Barkhausen noise analyses of stress in steel. Curr Appl Phys 4:308–311
9. Davut K, Gür CH (2007) Monitoring the microstructural changes during tempering of quenched SAE 5140 steel by magnetic Barkhausen noise. J Nondestruct Eval 26:107–113
10. Hug A, Kleber X, Merlin J, Petitgand H (2005) Dual-phase steels characterization using magnetic Barkhausen noise measurements. Mater Sci Forum 500–501:639–646
11. Koo KM, Ng Dickon HL, Lo CCH (2003) Characterization of pearlite grains in plain carbon steel by Barkhausen emission. Mater Sci Eng A351:310–315
12. Gauthier J, Krause TW (1998) Measurement of residual stress in steel by MBN technique. NDT&E Int 31(1):23–31
13. Stefanita CG, Atherton DL, Clapham L (2000) Plastic versus elastic deformation effects on magnetic Barkhausen noise in steel. Acta Mater 48:3545–3551
14. Mandal K, Loukas ME, Corey A, Atherton DL (1997) Magnetic Barkhausen noise indications of stress concentrations near pits of various depths. J Magn Magn Mater 175:255–262
15. Cotterell M, Cassidy S, Tanner DA, Mészáros I (2004) Magnetic-acoustic emission for the characterization of ferritic stainless steel microstructural state. J Magn Magn Mater 271:381–389
16. Yamaura S, Furuya Y, Watanabe T (2001) The effect of grain boundary microstructure on Barkhausen noise in ferromagnetic materials. Acta Mater 49:3019–3027
17. Park DG, Kim CG, Hong JH (2000) Microstructural dependence of Barkhausen noise and magnetic relaxation in the weld HAZ of and RPV steel. J Magn Magn Mater 215–216:765–768
18. Saquet O, Chicois J, Vincent A (1999) Barkhausen noise from plain carbon steels: analysis of the influence of microstructure. Mater Sci Eng A269:73–82
19. Ceurter JS, Smith C, Ott R (2002) The Barkhausen noise inspection method for detecting grinding damage in gears. American Gear Manufacturers Association, Alexandria
20. del Conte EG, Terixeira JC, Campos MA, Piccolo HA, Oliva DAO, Rodrigues LR (2016) Barkhausen noise analysis as an alternative method to online monitoring of milling surfaces. IEEE Trans Magn 52(5):1–4
21. Stupakov A, Neslušan M, Perevertov O (2016) Detection of a milling induced surface damage by the magnetic Barkhausen noise. J Magn Magn Mater 410:198–209
22. Rosipal M, Neslušan M, Ochodek V, Šípek M (2010) Application of Barkhausen noise for analysis of surface quality after machining. Mater Eng 17(2):11–14
23. Vashista M, Moorthy V (2013) Influence of applied magnetic field strength and frequency response of pick-up coil on the magnetic Barkhausen noise profile. J Magn Magn Mater 345:208–214
24. Vashista M, Moorthy V (2015) On the shape of the magnetic Barkhausen noise profile for better revelation of the effect of microstructures on the magnetisation process in ferritic steels. J Magn Magn Mater 393:584–592
25. Blažek D, Neslušan M, Mičica M, Pištora J (2016) Extraction of Barkhausen noise from the measured raw signal in high-frequency regimes. Measurement 94:456–463
26. Perez-Benitez JA, Capo-Sánchez J, Anglada-Rivera J, Padovese LR (2005) A model for the influence of microstructural defects on magnetic Barkhausen noise in plain steels. J Magn Magn Mater 288:433–442
27. Chávez-González AF, Pérez-Benítez JA, Espina-Hernández JH, Grössinger R, Hallen JM (2016) Influence of frequency of the excitation magnetic field and material's electric conductivity on domain wall dynamics in ferromagnetic materials. J Magn Mater 401:287–295
28. Gavin HP (2013) The Levenberg-Marquardt method for nonlinear least squares curve-fitting problems©
29. Bertotti G (1986) Some considerations on the physical interpretation of eddy current losses in ferromagnetic materials. J Magn Magn Mater 54–57:1556–1560
30. Fitzpatrick ME, Fry AT, Holdway P, Kandil FA, Shackleton J, Suominen L (2005) Determination of residual stress by X-ray diffraction—a national measurement good practise, Guide no. 52, ISSN 1744-3911
31. Bertoti G, Fiorillo F, Mazzetti P (1992) Basic principles of magnetization processes and origin of losses in soft magnetic materials. J Magn Magn Mater 112:146–149